

# CA-MoE: Channel-Adapted MoE for Incremental Weather Forecasting

Hao Chen<sup>1</sup> Han Tao<sup>1</sup> Guo Song<sup>1\*</sup> Jie Zhang<sup>1</sup> Yunlong Yu<sup>2</sup>  
Yonghan Dong<sup>3</sup> Chuang Yang<sup>4</sup> Lei Bai<sup>5\*</sup>

<sup>1</sup>Hong Kong University of Science and Technology(HKUST) <sup>2</sup>Zhejiang University

<sup>3</sup>Huawei Technologies Ltd. <sup>4</sup>PolyU <sup>5</sup>Shanghai AI Laboratory

\* Corresponding author hchener@connect.ust.hk

## Abstract

Atmospheric science is intricately connected with other fields, e.g., geography and aerospace. Most existing approaches involve training a joint atmospheric and geographic model from scratch, which incurs significant computational costs and overlooks the potential for incremental learning of weather variables across different domains. In this paper, we introduce incremental learning to weather forecasting and propose a novel structure that allows for the flexible expansion of variables within the model. Specifically, our method presents a Channel-Adapted MoE (CA-MoE) that employs a divide-and-conquer strategy. This strategy assigns variable training tasks to different experts by index embedding and reduces computational complexity through a channel-wise Top-K strategy. Experiments conducted on the widely utilized ERA5 dataset reveal that our method, utilizing only approximately 15% of trainable parameters during the incremental stage, attains performance that is on par with state-of-the-art competitors. Notably, in the context of variable incremental experiments, our method demonstrates negligible issues with catastrophic forgetting.

## 1. Introduction

With the rapid development of AI, AI4Weather [3, 6, 18] has emerged as one of the most significant fields within AI for science, achieving remarkable performance. This success is partly due to the availability of extensive training data and large-parameter models. Similar to the significant advancements observed in computer vision and natural language processing [5, 17], scaling up models is also beneficial in weather forecasting. Recent AI-based methods [3, 6] have outperformed traditional numerical weather prediction techniques [2] in various areas of atmospheric prediction.

Atmospheric variables are undeniably interconnected with other natural sciences, e.g., geography and aerospace. Many variables often overlooked in atmospheric science,

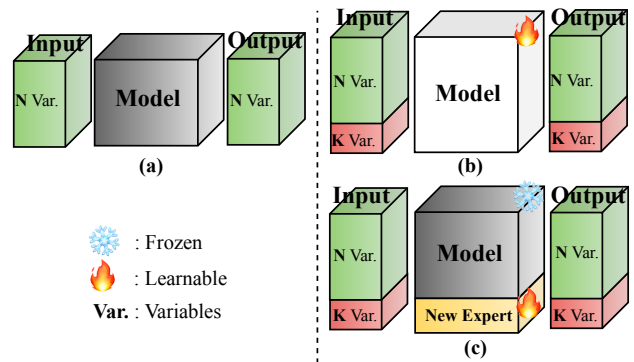


Figure 1. Comparison between the conventional approach (b) and our incremental structure (c). (a) represents training a model with N variables. (b) represents training a new model with N+K variables from scratch. (c) represents incremental training a model from N variables to N+K variables.

e.g., surface pressure and sea-level pressure, may hold significant relevance in these fields. To leverage the complementary effects of different variables, many studies opt to concatenate these variables and train a model from scratch, as illustrated in Fig. 1(b). Each time new variables are introduced, the model requires complete retraining due to the updated structure and parameters. This approach does not align with the way humans learn new knowledge and may result in an unnecessary training burden.

In this paper, a novel task termed **Incremental Weather Forecasting** is introduced, involving the dynamic expansion of variables with minimal parameter adjustments. While this approach shows promise in reducing the computational burden of full training, it grapples with a significant challenge known as *catastrophic forgetting*. This phenomenon occurs when the training components adapt to the distribution of newly introduced variables at the expense of forgetting the distribution of the original variables. To tackle this issue, this paper presents a network with the **Channel-Adapted MoE (CA-MoE)**, where new experts are integrated to capture the distribution of the newly added

variables, while the existing experts remain frozen.

**Incremental Weather Forecasting.** It is obviously that training a model from scratch is both tedious and costly, leading to a high computational burden in practice. To reduce the cost of adapting atmospheric models to other fields, it is crucial to explore incremental weather forecasting. As illustrated in Fig. 1, this task involves a two-stage process. Initially, specific variables are trained in the first stage, followed by incremental training of newly added variables in a subsequent phase. During the incremental stage, the experts from the first stage are frozen to minimize computational costs while preserving variable affinity.

**CA-MoE.** Although traditional MoE structures offer robust representational capabilities, their parallel structure with equally weighted experts tends to lead to homogenization. To address this issue, this paper introduces a structure called CA-MoE. CA-MoE assigns different experts to learn various variables, training some experts initially and introducing additional experts in the incremental stage to manage new variables. To ensure diversity among the experts, CA-MoE employs variable index embedding, which provides position information to guide experts in acquiring distinct knowledge. During training, this embedding selects the most relevant channels for learning different variables, thus reducing the computational burden. Unlike other MoE structures that select the most relevant expert only during inference, CA-MoE selects channels during both training and inference, effectively reducing computational costs in both stages.

In addition to the framework, we introduce a **variable-adapted loss function** designed to optimize the training speed of variables. Besides, a trainable loss weight is assigned to each variable, allowing for the regulation of the loss value.

In conclusion, the contributions of this work include:

- To the best of our knowledge, this study marks the pioneering investigation into incremental learning in weather forecasting. This paper introduces a novel benchmark aimed at assessing the impact of incremental weather modeling.
- This paper presents a novel framework for addressing the task of incremental weather modeling, termed the Channel-Adapted MoE (CA-MoE). The CA-MoE module assigns different experts to distinct variables, thereby reducing computational load by selectively activating relevant channels during both training and inference phases.
- In the incremental stage, our method requires finetuning only about 15% of the parameters to achieve performance comparable to some SOTA competitors in predicting surface variables, while also providing superior prediction performance for upper-air variables.

## 2. Related work

### 2.1. Data-Driven Weather Forecasting

In recent decades, traditional numerical weather prediction (NWP) [2] methods have dominated the field of weather forecasting due to their robust prediction results and rigorous mathematical validation. However, NWP methods [22,27] require training from scratch for each new prediction, resulting in slow computation and high costs.

With the rapid advancement of artificial intelligence and deep learning, researchers have increasingly explored data-driven methods for midterm weather forecasting. FourCastNet [18] pioneered this approach by utilizing Fourier Neural Operators (FNO) [20] to model weather datasets. Alternatively, Pangu-Weather [3] employs a 3D transformer [10,21] architecture to learn atmospheric data distributions. Building on these foundations, many teams have developed data-driven models using Neural Operators [4,20,33] or Neural Networks [6,7,19,38], achieving comparable or superior prediction accuracy to traditional NWP methods while reducing inference time and computational costs.

Like these approaches, our work introduces a novel network for weather prediction. While existing methods can predict future atmospheric variables at different pressure levels after a single training session, *the substantial training costs and fixed number of variables limit their applicability to other atmospheric prediction tasks.* Our work proposes a novel structure to explore incremental weather forecasting, enabling more flexible and efficient model expansion.

### 2.2. Incremental Learning

As deep learning progresses, researchers are exploring ways to transfer models from one domain to another while fine-tuning only a few parameters. One approach is incremental learning, which aims to learn new concepts while retaining the representational capacity of the initial dataset. Given the domain variations in incremental data, previous work in incremental learning has primarily focused on addressing Class Incremental Learning [12,16,29,40] or Task Incremental Learning [24,28,31,35,37]. Efforts in this field have involved developing various architectures to transfer the representative space from one task or dataset to others.

One of the most popular structures for addressing incremental learning tasks is the Mixture of Experts (MoE) model [14], which learns representations of new concepts through different experts. Due to its sparse architecture, many works have adopted the MoE structure to reduce inference costs and enhance model capacity [32,36]. An early work introducing MoE to incremental learning is Expert Gate [1], which trains multiple backbones as different experts and assigns new domains to the relevant expert. Lifelong-MoE [8] leverages pretrained experts and gates to retain the representational knowledge of the training do-

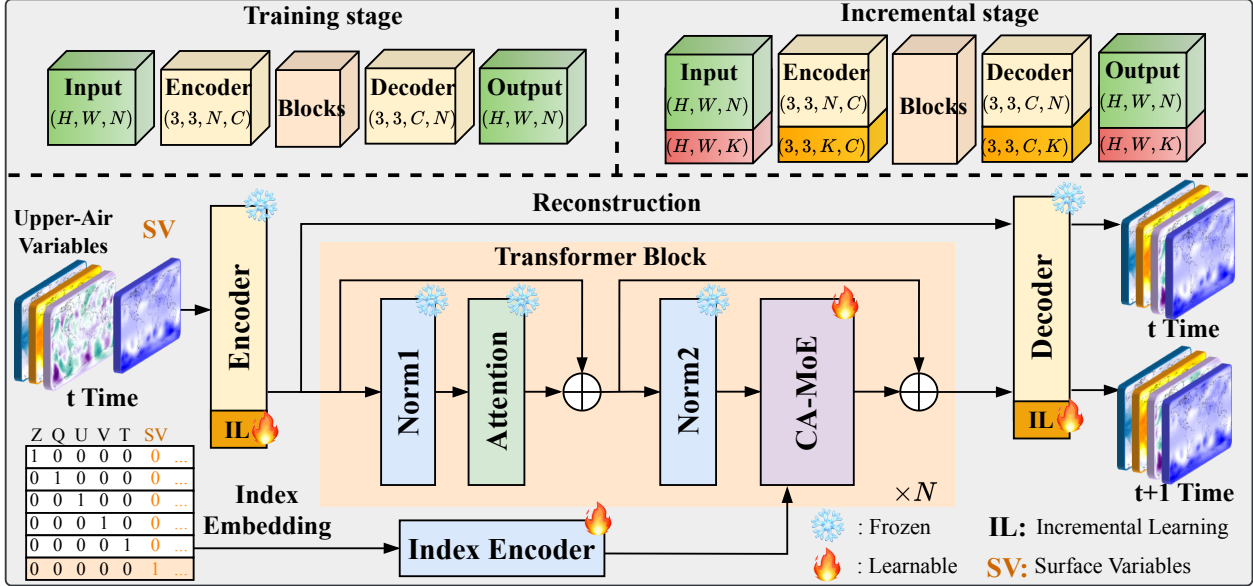


Figure 2. Illustration of the entire model. During the training stage, the model is trained using upper-air variables. In the incremental stage, the **fire** components are trained while the **snow** components remain frozen. The index embedding is trained concurrently within the Index Encoder and is divided into six parts in the CA-MoE module based on the variables.

main. In addition to these approaches, MoE is used as an adapter in MoE-Adapter [39], where adapters are attached to the main structure. These works have demonstrated the promising performance of MoE in visual and natural language incremental learning.

Unlike the previous MoE structure, which focus on a fixed number of variables, atmospheric variables are transformable due to variations in atmospheric pressure and types. Our work aims to incremental learn the distribution of atmospheric variables across different types, with various pressures assigning to multiple experts. *While previous works in incremental learning have focused on transferring models between tasks or datasets, our approach involves training model with incremental variables.*

### 3. Task Definition

Considering the novel task that we proposed in this work, we would like to introduce the definition at first. The weather variables  $\mathcal{X}^t$  are divided into the upper-air variables  $\mathcal{X}_h^t = \{X_Z^t, X_Q^t, X_U^t, X_V^t, X_T^t\}$  and the surface variables  $\mathcal{X}_{sv}^t$ , where  $t$  denotes the time,  $h$  denotes the upper-air variables,  $sv$  denotes the surface variables, and  $Z, Q, U, V, T$  denotes various types of upper-air variables. If we set  $\phi$  as the weather model to predict the future weather variables, the prediction process can be represented as  $\mathcal{X}^{t+1} = \phi(\mathcal{X}^t)$ .

Different from the previous weather prediction setting, our structure adopts the pretrain-incremental strategy, where pretraining the whole model with upper-air variables

and finetuning a few parameters with surface variables. Thus, the training process is divided into two stages. In the first stage, the upper-air variables are used to train a weather model, *i.e.*,  $\mathcal{X}_h^{t+1} = \phi(\mathcal{X}_h^t)$ . In the second stage, the upper-air variables and the surface variables are concatenated together to incremental train the model with a limited number of parameters, *i.e.*,  $\mathcal{X}_h^{t+1} + \mathcal{X}_{sv}^{t+1} = \phi_f(\mathcal{X}_h^t + \mathcal{X}_{sv}^t)$ , where  $\phi_f$  denotes finetuning a few parameters of model  $\phi$ .

## 4. Method

### 4.1. Framework

The primary objective of Incremental Weather modeling is to accurately represent the distribution of various atmospheric variables. This paper introduces a novel framework that addresses this task using a Channel-Adapted MoE (CA-MoE) to learn representations of different variables. As shown in Fig. 2, the proposed approach is divided into two stages: the training stage and the incremental stage. **In the training stage**, multiple experts are trained to capture the distribution of various upper-air variables. **During the incremental stage**, the pretrained experts and attention structures are frozen, while newly added experts are trained to incorporate the representation space of additional surface variables.

In addition to the main framework, several unique design elements are incorporated into the loss function to enhance performance. 1) Unlike traditional weather modeling structures, this work introduces **an additional trainable branch to reconstruct input atmospheric variables**, alongside a

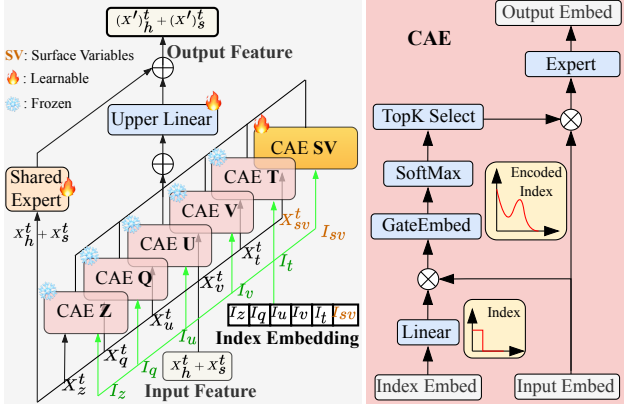


Figure 3. Illustration of the proposed Channel-Adapted MoE (CA-MoE). As depicted in the coordinate curves, the index embedding is discrete before encoding. After passing through the GateEmbed layer, the encoded index becomes continuous, reflecting the relevant channels associated with the variables.

prediction branch for forecasting future atmospheric variables. 2) To account for varying training speeds of different variables, a trainable loss weighting mechanism is implemented, allowing for the adjustment of training rates for each variable.

The CA-MoE is the key design in our framework, which will be introduced in detail.

## 4.2. Channel-Adapted MoE

This work introduces a novel structure, termed CA-MoE, tailored for the incremental learning of weather modeling. Unlike previous approaches that automatically determine expert selection preferences using auxiliary loss, CA-MoE incorporates an additional index-embedding to guide experts in learning variable affinity. This means that the relationships between experts and variables are preliminarily defined within the CA-MoE. When new variables are introduced, only a few experts need to be added. To reduce the computational complexity of CA-MoE, this work employs a topK selection layer. The layer reduces the number of channels in MoE during both the training and inference stages.

**Variables and Index Embedding.** As illustrated in Fig. 3, during the training stage, the input feature  $X_h^t \in \mathbb{R}^{65 \times H \times W}$  consists of five different types of variables:  $X_Z^t, X_Q^t, X_U^t, X_V^t, X_T^t \in \mathbb{R}^{13 \times H \times W}$ , where, 65 and 13 represent the number of variables, while (H) and (W) denote the spatial resolution. These five types of variables are concatenated and processed by a shared expert and five distinct Channel-Adapted Experts (CAEs). In addition to these variables, the framework introduces an extra one-hot index embedding  $I_h \in \mathbb{R}^{65 \times 5}$  to guide experts in learning variable affinity. The number 65 corresponds to the number of variables, and 5 corresponds to the number of variable types. Similar to the input weather features, the in-

dex embedding is composed of five separate embeddings:  $I_Z, I_Q, I_U, I_V, I_T \in \mathbb{R}^{65 \times 1}$ . This initial index embedding is then encoded into a latent space using a Linear layer, expressed as  $I_h = Linear(I_h)$ .

**Channel-Adapted Expert (CAE).** For upper-air variables, the operation remains consistent across different experts. Taking variable Z as an example, the input weather feature includes all five upper-air variables, and the index embedding is  $I_Z$ . This process can be formulated:

$$\mathbf{X}_Z^{t,CAE} = CAE_Z(X_h^t, I_Z), \quad (1)$$

where  $CAE_Z$  represents the CAE specific to the Z variable.

In each CAE module, the index embedding  $I_Z$  is encoded by a linear layer and then multiplied channel-wise with the input embedding  $X_h^t$ . The resulting fused feature is processed by the GateEmbed layer to produce a gate embedding, which enhances the fusion of the index and variable embeddings. This enhanced feature is then normalized using a SoftMax layer and filtered through a TopK layer to generate the GateIndex  $GI_Z \in \mathbb{R}^{K \times H \times W}$  and GateWeight  $GW_Z \in \mathbb{R}^{K \times H \times W}$ , where the top-K high-rank channels are selected. The process is expressed as:

$$GI_Z, GW_Z = TopK(SoftMax(GE_Z(X_h^t, I_Z))), \quad (2)$$

where  $GE_Z$  denotes the GateEmbed layer for the Z variable. Once the GateIndex and GateWeight are obtained, the index selection is applied to the input embedding guided by the GateIndex, while the channel-wise weighting of the variable embedding is performed by the GateWeight. This selected and weighted embedding contributes to reducing the computational cost of subsequent modules. The process is formulated as:

$$\mathbf{X}_Z^{t,selected} = GW_Z * Select_Z(X_h^t, GI_Z), \quad (3)$$

where  $Select_Z$  denotes the selection function within the  $CAE_Z$  module.

The selected and weighted embedding represents the key features associated with the specific type of variables. In the  $CAE_Z$  module, these features serve as the training set for learning the distribution of the Z variable with  $Expert_Z$ . The expert module employs a parallel structure, dividing the channels into several parts and enhancing each part with a sparse Mixture of Experts (MoE). This process is:

$$\mathbf{X}_Z^{t,CAE} = Expert_Z(\mathbf{X}_Z^{t,selected}). \quad (4)$$

**Shared Expert.** The shared expert extracts the overall features from all channels and operates in parallel with several CAE modules. Each type of variable is processed by its corresponding CAE module, and their outputs are summed to obtain the fused features  $X_h^{t,fused}$  for all variable types. Since the channel count of the selected variable embeddings

is lower than that of the original embeddings, an additional up-channel linear layer,  $Linear_{up}$ , is introduced. The fused feature and the output from the shared expert are then combined through pixel-wise addition. This process is:

$$\mathbf{X}_h^{t,fused} = CAE_Z(X_h^t, I_Z) + \dots + CAE_T(X_h^t, I_T), \quad (5)$$

$$(\mathbf{X}')_h^t = Expert_{shared}(X_h^d) + Linear_{up}(X_h^{d,fused}). \quad (6)$$

**There are several notable aspects of CA-MoE.** 1) The GateEmbed layer leverages variable embeddings to drive the index embedding, facilitating the generation of a variable-specific confidence matrix. Within the CAE module, this embedding enriches the content of the confidence matrix by integrating both semantic and positional information, in contrast to previous iterations that relied solely on positional information. 2) Unlike prior methodologies that assign different experts to reduce computational costs during inference, this study simplifies computational complexity by eliminating low-relevance channels. This approach effectively reduces computational costs in both the training and inference phases. 3) Why does this work not assign different variables to experts directly? Although variables of different types exhibit strong interrelations, they are fused across multiple module blocks. Furthermore, the additional index embedding assists in selecting the most relevant channels, thereby maximizing the extraction of semantic information.

### 4.3. Incremental Modeling

In the incremental stage, this work requires only minor parameter adjustments to adapt the model from one domain to another. Several operations are necessary within the encoder, decoder, and CA-MoE modules.

**In the Encoder and Decoder modules,** the parameters are reorganized to accommodate different variables according to their specific indices. As illustrated in Fig. 2, both the Encoder and Decoder contain channel mappings from the number of variables  $N$  to the channels of the latent space  $C$ , resulting in a convolutional layer shape of  $(3, 3, N, C)$ . When the number of variables increases to  $N + K$  in the incremental stage, the shape changes to  $(3, 3, N + K, C)$ . The parameters of the convolutional layer are divided into two parts based on the positions of the variables: the  $(3, 3, N, C)$  portion is initialized with pre-trained parameters, while the  $(3, 3, K, C)$  portion is initialized randomly. The initialization method for the position embedding and the Decoder module follows the same approach.

**In the CA-MoE module,** new CAE structures are introduced to learn the distribution of newly added variables. The newly added expert is tasked with learning this distribution and operates in parallel with the other experts. During the incremental stage, only the newly added expert and the shared expert are trained, while the other experts remain frozen.

### 4.4. Training Loss

To assess the similarity between the predicted results and the ground truth, this work employs the L2 loss function to guide the optimization process. Unlike previous approaches, this work incorporates unique features in the loss function, including reconstruction loss and dynamic loss.

**Dynamic Loss.** To account for the unique characteristics of weather variables, this work treats the prediction of each variable as an individual task by introducing trainable weights that dynamically adjust the training speed for each variable. In the incremental stage, the loss weight for pretrained variables is set lower than that for newly added variables. *This approach helps maintain the model affinity of the pretrained variables while fully training the newly added variables.* The process can be expressed as:

$$\mathbf{L} = (\hat{X}^{t+1} - X^{t+1})^2 / e^w + w, \quad (7)$$

where  $\hat{X}^{t+1}, X^{t+1} \in \mathbb{R}^{C \times H \times W}$  represent the predicted results and the ground truth, respectively, and  $w \in \mathbb{R}^C$  denotes the loss weight for each variable.

**Reconstruction Loss.** To fully leverage the predictive capabilities of the transformer blocks, this work introduces an additional reconstruction branch that reconstructs the input variables  $\mathcal{X}^t$  by generating the reconstructed variables  $\hat{\mathcal{X}}^t$ . In this design, the Encoder and Decoder modules are responsible for encoding and reconstructing, while the intermediate blocks handle the prediction task. *The reconstruction loss ensures that the transformer blocks do not need to participate in the decoder module.* The reconstruction loss and the prediction loss are jointly trained with a hyperparameter  $\lambda$ . The process is formulated as follows:

$$\text{Loss} = L_p + \lambda L_r, \quad (8)$$

where  $L_p$  and  $L_r$  denote the prediction loss and reconstruction loss, respectively.

## 5. Experiments

**Dataset.** In this work, we conduct experiments on a popular weather dataset, *i.e.*, ERA5 [13], provided by the ECMWF. ERA5 dataset is a reanalysis atmospheric dataset, consisting of the atmospheric variables from 1979 to the present day with a  $0.25^\circ$  spatial resolution with  $721 \times 1440$ . Considering the computation cost, this work uses the dataset with a  $1.4^\circ$  spatial resolution by downsampling the variables to  $128 \times 256$ . Same as the previous works, we train the model on 40-year dataset, which contains the weather variables from 1979 to 2020 year, and test the model on one-year dataset of weather variables in 2021. In this work, the model processes 5 upper-air variables and 3 surface variables as Tab. 1, where the upper-air variables are exploited in the training stage, and the surface variables are exploited in the incremental learning stage.

Name	Description	Levels
<b>Upper-Air</b>		
Z	Geopotential	13
Q	Specific humidity	13
U	x-direction wind	13
V	y-direction wind	13
T	Temperature	13
<b>Surface-Incremental Learning</b>		
u10	x-direction wind at 10m height	Single
v10	y-direction wind at 10m height	Single
t2m	Temperature at 2m height	Single
msl	Mean sea-level pressure	Single
sp	Surface pressure	Single

Table 1. A summary of atmospheric variables. The 13 levels are 50, 100, 150, 200, 250, 300, 400, 500, 600, 700, 850, 925, 1000 hPa. ‘Single’ denotes the variables under earth’s surface.

**Implementation Details.** The main structure of this work follows the backbone of ViT [10], Swin Transformer [21], and Flash Attention [9]. We apply the AdamW optimizer with 0.0002 and 0.00005 learning rates to train the model in training and incremental learning stages, respectively. In both training and incremental learning stages, we train 100 epochs and set batch size to 16. Our model is trained on the PyTorch with 16 NVIDIA Tesla A100 GPUs. The codes would be released.

**Ablation study is presented in Supplementary Material.**

### 5.1. Incremental Surface Variables prediction

In this work, we evaluate our model on three surface variables: T2M, U10, and V10. **Notably, our approach is the only one tested in an incremental learning setting, while all other methods are evaluated using standard training.** Although the number of trainable parameters in our model is lower, approximately 30% of the parameters used in the plain ViT [10], the CA-MoE model outperforms the baseline across all three time periods: 6 hours, 72 hours, and 120 hours. For T2M, the RMSE of CA-MoE is lower than that of the baseline by nearly 2.7K in the 6-hour, 72-hour, and 120-hour predictions. For U10 and V10, the RMSE of CA-MoE is reduced by approximately 2.8 m/s in the 6-hour prediction and by around 3.8 m/s in both the 72-hour and 120-hour predictions. In comparison to other public methods, our work demonstrates comparable performance to Pangu-Weather [3] and outperforms IFS [22] and FourCastNet [18] across nearly all metrics. A detailed analysis will be provided in Sec. 5.3. We conclude that, **despite other methods being fully trained on the same dataset, our incremental model performs effectively in predicting surface variables.**

From Tab. 2, when we extend the incremental variables

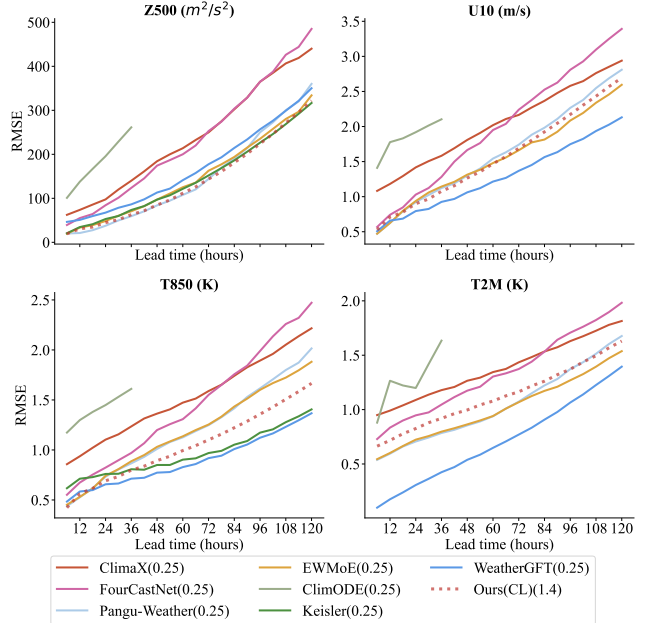


Figure 4. Comparative analysis of **RMSE ↓** across seven data-driven models for four variables, including Z500 and T850 (upper-air variables), as well as T2M and U10 (incremental surface variables). **The terms ‘0.25’ and ‘1.4’ refer to spatial resolutions of  $721 \times 1440$  and  $128 \times 256$ , respectively.**

to 5, there is no significant damping of T2M, U10, and V10. **The performance of msl and sp are presented in the Supplementary Material.**

### 5.2. Upper-Air Variables Prediction

In the field of upper-air variable prediction, we primarily compare our model against baselines and several publications, as shown in Tab. 3. Compared to the baselines with the same resolution, CA-MoE clearly outperforms both ViT [10] and ViT+MoE [25] in the same settings. Our method demonstrates superior performance across all prediction periods for the five types of upper-air variables when compared to the baselines and the IFS model [26] proposed by ECMWF. In comparison to Pangu-Weather, our work also achieves better performance in short-term predictions, although it is slightly less effective in the 72-hour and 120-hour predictions. A detailed analysis of the publications will be provided in Sec. 5.3.

In addition to comparing with other competitors, **it is essential to evaluate our model’s performance with and without incremental learning.** Although the experts associated with upper-air variables remain frozen during the incremental training stage, CA-MoE performs well in upper-air variable prediction. Following incremental training, CA-MoE(IL) shows slight improvements across all three periods and for all five upper-air variables. Notably, in long-term Z500 predictions, CA-MoE reduces the error by an additional 9.1 and 7.6  $m^2/s^2$  in the 72-hour and 120-hour

	Size	Num Var.	Para. (M)	T2M(K) ↓			U10(m/s) ↓			V10(m/s) ↓		
				6h	72h	120h	6h	72h	120h	6h	72h	120h
Plain Training with <b>all 68 Variables</b>												
IFS [26]	721*1440	-	-	1.093	1.384	1.737	0.963	1.874	2.777	0.986	1.926	2.872
pangu-weather [3]	721*1440	68	-	0.816	<u>1.094</u>	<b>1.534</b>	0.765	<b>1.629</b>	<b>2.544</b>	0.788	<b>1.684</b>	<b>2.648</b>
FourCastNet [18]	721*1440	68	-	0.823	<b>1.017</b>	1.765	0.815	2.080	3.339	0.837	2.106	3.410
ViT* [10]	128*256	68	306.6	0.831	1.421	1.908	0.806	2.054	3.076	0.825	2.103	3.185
Incremental Training from <b>65 Upper-air Variables</b> to <b>3 Surface Variables</b>												
CA-MoE(IL)	128*256	<b>68</b>	107.3	<b>0.663</b>	1.163	<u>1.630</u>	<b>0.526</b>	<u>1.689</u>	<u>2.694</u>	<b>0.533</b>	<u>1.734</u>	<u>2.770</u>
Incremental Training from <b>65 Upper-air Variables</b> to <b>5 Surface Variables</b>												
CA-MoE(IL)	128*256	<b>70</b>	107.3	<u>0.668</u>	1.166	1.639	<u>0.530</u>	1.699	2.709	<u>0.536</u>	1.743	2.791

Table 2. Prediction performances on Incremental Training task with 3 surface variables, *i.e.*, T2M, U10, and V10. \* denotes running by ourselves. The best and the second best results are marked in **bold** and underline, respectively.

	Para. (M)	Z500( $m^2/s^2$ ) ↓			Q500( $\times e^{-3}, g/kg$ ) ↓			U500( $m/s$ ) ↓			V500( $m/s$ ) ↓			T500(K) ↓		
		6h	72h	120h	6h	72h	120h	6h	72h	120h	6h	72h	120h	6h	72h	120h
<b>0.25° (721 × 1440)</b>																
IFS [22]	-	28.30	154.1	333.0	0.31	0.61	0.74	1.429	3.555	5.491	1.395	3.577	5.633	0.389	1.068	1.796
Pangu-weather [3]	-	29.24	<b>139.8</b>	<b>304.6</b>	0.27	<b>0.51</b>	<b>0.66</b>	1.335	<b>3.062</b>	<b>4.825</b>	1.319	<b>3.119</b>	<b>5.041</b>	0.381	<b>0.928</b>	<b>1.598</b>
<b>1.4° (128 × 256)</b>																
ViT* [10]	307	33.38	209.4	517.8	0.22	0.61	1.06	1.241	3.663	6.523	1.226	3.765	7.416	0.425	1.180	2.400
ViT+MoE(light)* [25]	609	37.92	207.1	405.7	0.22	0.60	0.78	1.304	3.842	5.878	1.276	3.896	6.105	0.461	1.237	2.028
ViT+MoE* [25]	1113	28.31	169.6	356.0	0.23	0.56	0.72	1.213	3.468	5.441	1.233	3.543	5.690	0.354	1.076	1.839
CA-MoE*	665	<u>21.44</u>	152.7	329.5	<u>0.18</u>	0.55	0.72	<u>0.902</u>	3.250	5.219	<u>0.904</u>	3.302	5.415	<u>0.276</u>	1.013	1.756
CA-MoE(IL)*	107	<b>19.32</b>	<u>143.6</u>	<u>321.9</u>	<b>0.18</b>	<u>0.54</u>	<u>0.71</u>	<b>0.899</b>	<u>3.225</u>	<u>5.185</u>	<b>0.900</b>	<u>3.276</u>	<u>5.388</u>	<b>0.271</b>	<u>0.980</u>	<u>1.722</u>

Table 3. Prediction performances on Training task with 5 upper-air variables under 500 hPa. \* denotes running by ourselves. The best and the second best results are marked in **bold** and underline, respectively.

predictions, respectively.

Thus, we conclude that our incremental method can effectively learn newly added variables with minimal parameter adjustments while also slightly enhancing the performance of the variables included in the initial training stage.

### 5.3. Comparison with State-of-the-Art

To evaluate the effectiveness of the proposed model, we conduct extensive comparisons with state-of-the-art (SOTA) competitors, including ClimaX [23], Pangu-Weather [3], ClimODE [30], WeatherGFT [34], FourCastNet [18], EWMoE [11], and Keisler [15]. Fig. 4 presents the quantitative comparison results for the 5-day weather prediction task, which is divided into two categories: upper-air variable prediction (T850 and Z500) and incremental learning for surface variable prediction (T2M and U10). It is important to note that all competitors are trained on a 0.25° weather dataset with a resolution of 721 × 1440, while our method is trained on a 1.4° weather dataset with a resolution of 128 × 256. From Fig. 4, it is evident that our incremen-

tal model performs comparably to some leading works in surface variable prediction.

**Upper-Air Variables.** For T850, our method is nearly the best in short-term prediction, performing on par with EWMoE [11] and Pangu-Weather [3], and surpassing WeatherGFT [34] and Keisler [15]. From the 18-hour mark onward, our work outperforms both EWMoE [11] and Pangu-Weather [3], although it performs worse than WeatherGFT [34] and Keisler [15] in long-term predictions. For Z500, our model achieves one of the best performances among all eight methods, outperforming Pangu-Weather [3] and WeatherGFT [34], and significantly exceeding ClimaX [23] and FourCastNet [18].

**Surface Variables (Incremental Learning).** Regarding surface variables, our model exhibits similar performance to Pangu-Weather [3] and EWMoE [11] for both T2M and U10. In comparison to FourCastNet [18], ClimODE [30], and ClimaX [23], our model demonstrates significant advantages in both short-term and long-term predictions. While it is slightly less effective than WeatherGFT [34], its

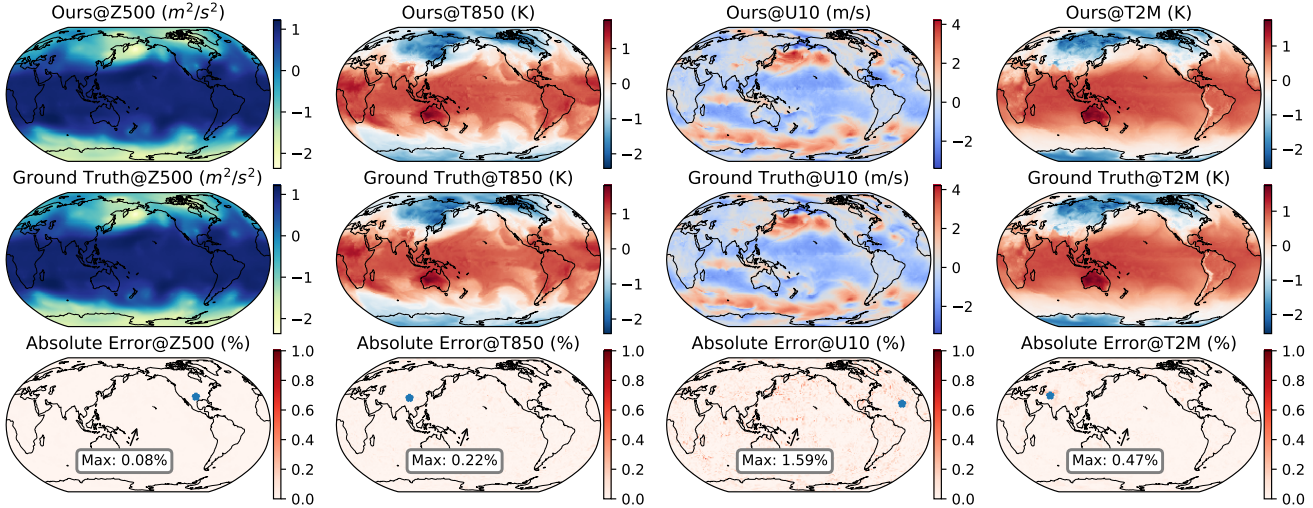


Figure 5. Some variables visualization of 6-hour global weather prediction.

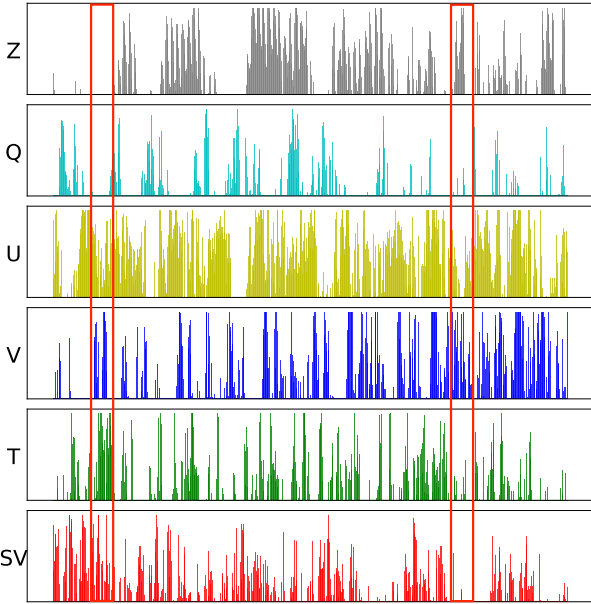


Figure 6. Frequency for selected Channels with different variables. ‘SV’ denotes the surface variables.

short-term prediction performance is comparable.

Despite having a smaller resolution size than recent methods, our work outperforms many state-of-the-art competitors, although it is slightly inferior to WeatherGFT [34]. Regarding incremental variables, our method achieves comparable performance to several top-tier fully trained models, while our incremental approach only fine-tunes less than 15% of the parameters. In conclusion, our method can flexibly transfer knowledge from upper-air variables to surface variables without encountering the problem of catastrophic forgetting in surface variables, making it more effective than recent weather forecasting methods.

## 5.4. Visualization

In the work, we visualize some predicted results and parameters. In Fig. 5, we visualize the 6-hour predicted results of Z500, T850, U10, and T2M. There are max 0.08%, 0.22%, 1.59%, and 0.47% absolute errors across 4 variables, including 2 upper-air variables and 2 surface variables. As shown in Fig. 6, we visualize the gate weights in the last block of 6 experts, including variables Z, Q, U, V, T, and SV. From the visualization, different channels are activated in different experts, which indicates the experts develop an affinity for different variables during the training process.

More visualized results are presented in Supplementary Material.

## 6. Conclusion

In this paper, we have proposed a novel task called incremental weather forecasting to explore the variable expansion capability of weather models. When new variables are incorporated, our approach obviates the necessity of training a model from scratch. Instead, we fine-tune a select number of parameters to adapt to the distribution of the newly introduced variables. To address this task, we introduce a novel structure called Channel-Adapted MoE (CA-MoE), which assigns different variables to various experts guided by index embedding. Experimental results demonstrate that the performance of the incremental model can be comparable performance to those of fully trained models. From the experimental results, we conclude that the incremental model can significantly reduce the computational costs associated with expanding the base weather model to other domains, avoiding the need for retraining from scratch.

## References

- [1] Rahaf Aljundi, Punarjay Chakravarty, and Tinne Tuytelaars. Expert gate: Lifelong learning with a network of experts. In *Proceedings of the IEEE conference on computer vision and pattern recognition*, pages 3366–3375, 2017. 2
- [2] Peter Bauer, Alan Thorpe, and Gilbert Brunet. The quiet revolution of numerical weather prediction. *Nature*, 525(7567):47–55, 2015. 1, 2
- [3] Kaifeng Bi, Lingxi Xie, Hengheng Zhang, Xin Chen, Xiaotao Gu, and Qi Tian. Accurate medium-range global weather forecasting with 3d neural networks. *Nature*, 619(7970):533–538, 2023. 1, 2, 6, 7
- [4] Boris Bonev, Thorsten Kurth, Christian Hundt, Jaideep Pathak, Maximilian Baust, Karthik Kashinath, and Anima Anandkumar. Spherical fourier neural operators: learning stable dynamics on the sphere. In *Proceedings of the 40th International Conference on Machine Learning*, 2023. 2
- [5] Tom B Brown. Language models are few-shot learners. *arXiv preprint arXiv:2005.14165*, 2020. 1
- [6] Kang Chen, Tao Han, Junchao Gong, Lei Bai, Fenghua Ling, Jing-Jia Luo, Xi Chen, Leiming Ma, Tianning Zhang, Rui Su, et al. Fengwu: Pushing the skillful global medium-range weather forecast beyond 10 days lead. *arXiv preprint arXiv:2304.02948*, 2023. 1, 2
- [7] Lei Chen, Xiaohui Zhong, Feng Zhang, Yuan Cheng, Yinghui Xu, Yuan Qi, and Hao Li. Fuxi: A cascade machine learning forecasting system for 15-day global weather forecast. *npj Climate and Atmospheric Science*, 6(1):190, 2023. 2
- [8] Wuyang Chen, Yanqi Zhou, Nan Du, Yanping Huang, James Laudon, Zhifeng Chen, and Claire Cui. Lifelong language pretraining with distribution-specialized experts. In *International Conference on Machine Learning*, pages 5383–5395. PMLR, 2023. 2
- [9] Tri Dao, Dan Fu, Stefano Ermon, Atri Rudra, and Christopher Ré. Flashattention: Fast and memory-efficient exact attention with io-awareness. *Advances in Neural Information Processing Systems*, 35:16344–16359, 2022. 6
- [10] Alexey Dosovitskiy. An image is worth 16x16 words: Transformers for image recognition at scale. *arXiv preprint arXiv:2010.11929*, 2020. 2, 6, 7
- [11] Lihao Gan, Xin Man, Chenghong Zhang, and Jie Shao. Ew-moe: An effective model for global weather forecasting with mixture-of-experts. *arXiv preprint arXiv:2405.06004*, 2024. 7
- [12] Dipam Goswami, Albin Soutif-Cormerais, Yuyang Liu, Sandesh Kamath, Bart Twardowski, Joost van de Weijer, et al. Resurrecting old classes with new data for exemplar-free continual learning. In *Proceedings of the IEEE/CVF Conference on Computer Vision and Pattern Recognition*, pages 28525–28534, 2024. 2
- [13] Hans Hersbach, Bill Bell, Paul Berrisford, Shoji Hirahara, András Horányi, Joaquín Muñoz-Sabater, Julien Nicolas, Carole Peubey, Raluca Radu, Dinand Schepers, et al. The era5 global reanalysis. *Quarterly Journal of the Royal Meteorological Society*, 146(730):1999–2049, 2020. 5
- [14] Robert A Jacobs, Michael I Jordan, Steven J Nowlan, and Geoffrey E Hinton. Adaptive mixtures of local experts. *Neural computation*, 3(1):79–87, 1991. 2
- [15] Ryan Keisler. Forecasting global weather with graph neural networks. *arXiv preprint arXiv:2202.07575*, 2022. 7
- [16] Beomyoung Kim, Joonsang Yu, and Sung Ju Hwang. Eclipse: Efficient continual learning in panoptic segmentation with visual prompt tuning. In *Proceedings of the IEEE/CVF Conference on Computer Vision and Pattern Recognition (CVPR)*, pages 3346–3356, June 2024. 2
- [17] Alexander Kirillov, Eric Mintun, Nikhila Ravi, Hanzi Mao, Chloe Rolland, Laura Gustafson, Tete Xiao, Spencer Whitehead, Alexander C. Berg, Wan-Yen Lo, Piotr Dollar, and Ross Girshick. Segment anything. In *Proceedings of the IEEE/CVF International Conference on Computer Vision (ICCV)*, pages 4015–4026, 2023. 1
- [18] Thorsten Kurth, Shashank Subramanian, Peter Harrington, Jaideep Pathak, Morteza Mardani, David Hall, Andrea Miele, Karthik Kashinath, and Anima Anandkumar. Four-castnet: Accelerating global high-resolution weather forecasting using adaptive fourier neural operators. In *Proceedings of the Platform for Advanced Scientific Computing Conference, PASC '23*, 2023. 1, 2, 6, 7
- [19] Remi Lam, Alvaro Sanchez-Gonzalez, Matthew Willson, Peter Wirnsberger, Meire Fortunato, Ferran Alet, Suman Ravuri, Timo Ewalds, Zach Eaton-Rosen, Weihua Hu, et al. Learning skillful medium-range global weather forecasting. *Science*, 382(6677):1416–1421, 2023. 2
- [20] Zongyi Li, Nikola Kovachki, Kamyar Azizzadenesheli, Burigede Liu, Kaushik Bhattacharya, Andrew Stuart, and Anima Anandkumar. Fourier neural operator for parametric partial differential equations. *arXiv preprint arXiv:2010.08895*, 2020. 2
- [21] Ze Liu, Yutong Lin, Yue Cao, Han Hu, Yixuan Wei, Zheng Zhang, Stephen Lin, and Baining Guo. Swin transformer: Hierarchical vision transformer using shifted windows. In *Proceedings of the IEEE/CVF International Conference on Computer Vision (ICCV)*, pages 10012–10022, 2021. 2, 6
- [22] Franco Molteni, Roberto Buizza, Tim N Palmer, and Thomas Petrolia. The ecmwf ensemble prediction system: Methodology and validation. *Quarterly journal of the royal meteorological society*, 122(529):73–119, 1996. 2, 6, 7
- [23] Tung Nguyen, Johannes Brandstetter, Ashish Kapoor, Jayesh K. Gupta, and Aditya Grover. Climax: A foundation model for weather and climate. In *International Conference on Machine Learning*, 2023. 7
- [24] Youqi Pan, Wugen Zhou, Yingdian Cao, and Hongbin Zha. Adaptive vio: Deep visual-inertial odometry with online continual learning. *arXiv preprint arXiv:2405.16754*, 2024. 2
- [25] Byeongjun Park, Hyojun Go, Jin-Young Kim, Sangmin Woo, Seokil Ham, and Changick Kim. Switch diffusion transformer: Synergizing denoising tasks with sparse mixture-of-experts. *European Conference on Computer Vision*, 2024. 6, 7

- [26] D Richardson. The thorpex interactive grand global ensemble (tigge). In *Geophys. Res. Abstr.*, volume 7, page 02815, 2005. 6, 7
- [27] Harold Ritchie, Clive Temperton, Adrian Simmons, Mariano Hortal, Terry Davies, David Dent, and Mats Hamrud. Implementation of the semi-lagrangian method in a high-resolution version of the ecmwf forecast model. *Monthly Weather Review*, 123(2):489–514, 1995. 2
- [28] Minhyuk Seo, Hyunseo Koh, Wonje Jeung, Minjae Lee, San Kim, Hankook Lee, Sungjun Cho, Sungik Choi, Hyunwoo Kim, and Jonghyun Choi. Learning equi-angular representations for online continual learning. In *Proceedings of the IEEE/CVF Conference on Computer Vision and Pattern Recognition*, pages 23933–23942, 2024. 2
- [29] Yuwen Tan, Qin hao Zhou, Xiang Xiang, Ke Wang, Yuchuan Wu, and Yongbin Li. Semantically-shifted incremental adapter-tuning is a continual vitransformer. In *Proceedings of the IEEE/CVF Conference on Computer Vision and Pattern Recognition*, pages 23252–23262, 2024. 2
- [30] Yogesh Verma, Markus Heinonen, and Vikas Garg. ClimODE: Climate forecasting with physics-informed neural ODEs. In *The Twelfth International Conference on Learning Representations*, 2024. 7
- [31] Maorong Wang, Nicolas Michel, Ling Xiao, and Toshihiko Yamasaki. Improving plasticity in online continual learning via collaborative learning. In *Proceedings of the IEEE/CVF Conference on Computer Vision and Pattern Recognition*, pages 23460–23469, 2024. 2
- [32] Jialin Wu, Xia Hu, Yaqing Wang, Bo Pang, and Radu Soricut. Omni-smola: Boosting generalist multimodal models with soft mixture of low-rank experts. In *Proceedings of the IEEE/CVF Conference on Computer Vision and Pattern Recognition*, pages 14205–14215, 2024. 2
- [33] Wei Xiong, Muyuan Ma, Xiaomeng Huang, Ziyang Zhang, Pei Sun, and Yang Tian. Koopmanlab: machine learning for solving complex physics equations. *APL Machine Learning*, 1(3), 2023. 2
- [34] Wanghan Xu, Fenghua Ling, Wenlong Zhang, Tao Han, Hao Chen, Wanli Ouyang, and Lei Bai. Generalizing weather forecast to fine-grained temporal scales via physics-ai hybrid modeling. *Advances in Neural Information Processing Systems*, 2024. 7, 8
- [35] Hongwei Yan, Liyuan Wang, Kaisheng Ma, and Yi Zhong. Orchestrate latent expertise: Advancing online continual learning with multi-level supervision and reverse self-distillation. In *Proceedings of the IEEE/CVF Conference on Computer Vision and Pattern Recognition*, pages 23670–23680, 2024. 2
- [36] Yuqi Yang, Peng-Tao Jiang, Qibin Hou, Hao Zhang, Jinwei Chen, and Bo Li. Multi-task dense prediction via mixture of low-rank experts. In *Proceedings of the IEEE/CVF Conference on Computer Vision and Pattern Recognition*, pages 27927–27937, 2024. 2
- [37] Fei Ye and Adrian G Bors. Online task-free continual generative and discriminative learning via dynamic cluster memory. In *Proceedings of the IEEE/CVF Conference on Computer Vision and Pattern Recognition*, pages 26202–26212, 2024. 2
- [38] Demin Yu, Xutao Li, Yunming Ye, Baoquan Zhang, Chuyao Luo, Kuai Dai, Rui Wang, and Xunlai Chen. Diffcast: A unified framework via residual diffusion for precipitation nowcasting. In *Proceedings of the IEEE/CVF Conference on Computer Vision and Pattern Recognition*, pages 27758–27767, 2024. 2
- [39] Jiazuo Yu, Yunzhi Zhuge, Lu Zhang, Ping Hu, Dong Wang, Huchuan Lu, and You He. Boosting continual learning of vision-language models via mixture-of-experts adapters. In *Proceedings of the IEEE/CVF Conference on Computer Vision and Pattern Recognition*, pages 23219–23230, 2024. 3
- [40] Fei Zhu, Zhen Cheng, Xu-Yao Zhang, Cheng-Lin Liu, and Zhaoxiang Zhang. Rcl: Reliable continual learning for unified failure detection. In *Proceedings of the IEEE/CVF Conference on Computer Vision and Pattern Recognition*, pages 12140–12150, 2024. 2